

Assessment of the Nematocidal Activity of Metallocenyl Derivatives of Monepantel

Jeannine Hess,^a Malay Patra,^a Abdul Jabbar,^b Vanessa Pierroz,^{a,c} Sandro Konatschnig,^a Bernhard Spingler,^a Stefano Ferrari,^c Robin B. Gasser^{b,} and Gilles Gasser^{a,*}*

- ^a Department of Chemistry, University of Zurich, Winterthurerstrasse 190, CH-8057 Zurich, Switzerland.
- ^b Faculty of Veterinary and Agricultural Sciences, The University of Melbourne, Parkville, Victoria 3010, Australia.
- ^c Institute of Molecular Cancer Research, University of Zurich, Winterthurerstrasse 190, CH-8057 Zurich, Switzerland.

* Corresponding authors: Email: robinbg@unimelb.edu.au; WWW: <http://www.gasserlab.org/>; Tel. +61 3 9731 2283; Email: gilles.gasser@chem.uzh.ch; WWW: www.gassergroup.com; Tel.: +41 44 635 46 30.

Keywords: Anti-parasitic compounds, bioorganometallic chemistry, *H. contortus*, livestock industry, monepantel, organometallic medicinal chemistry.

Abbreviations: AADs – Amino-Acetonitrile Derivatives; *C. felis* – *Ctenocephalides felis*; *D. immitis* – *Dirofilaria immitis*; ESI-MS – Electrospray Ionisation-Mass Spectrometry; *H. contortus* – *Haemonchus contortus*; H2DCFDA – 2',7'-dichlorofluorescein diacetate; LDA – larval development assay; *L. cuprina* – *Lucilia cuprina*; nAChR – nicotinic acetylcholine receptor; o.n. – overnight; *P. falciparum* – *Plasmodium falciparum*; ROS – reactive oxygen species; *R. sanguineus* – *Rhipicephalus sanguineus*; r.t. – room temperature; SAR – Structure Activity Relationship; TBH – *tert*-butyl hydroperoxide; *T. colubriformis* – *Trichostrongylus colubriformis*.

Abstract

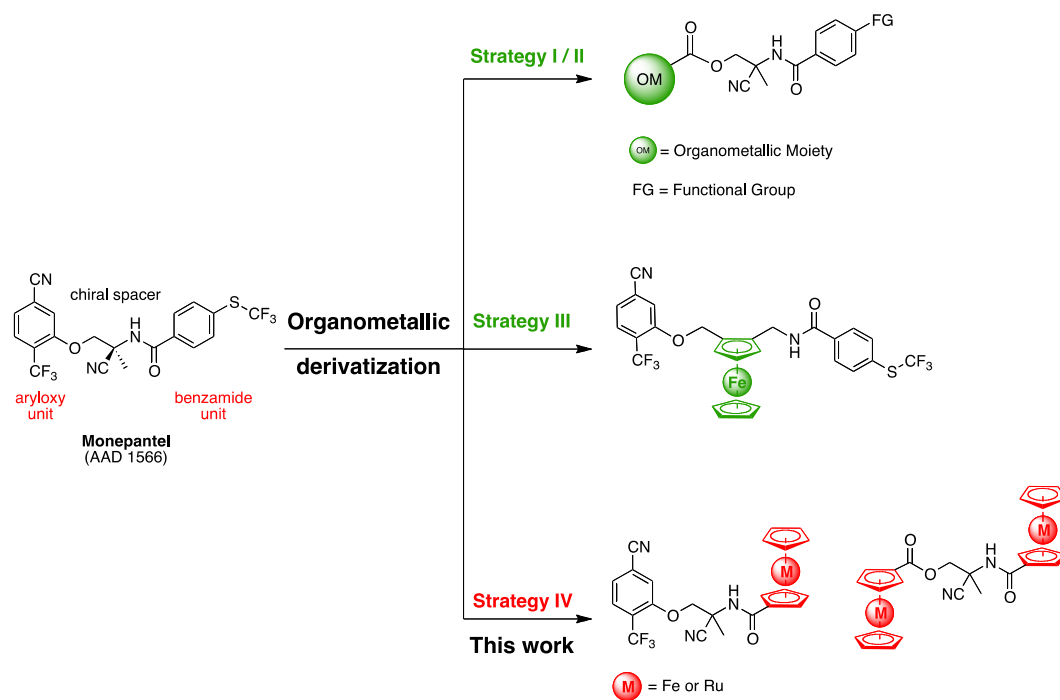
In this study, we present the design, synthesis, characterization and biological evaluation of structurally new ferrocenyl and ruthenocenyl derivatives of the recently launched organic anthelmintic monepantel (Zolvix[®]). All seven metallocenyl derivatives prepared (**4a/b**, **5a/b**, **6a/b** and **7**) were isolated as racemates and characterized by ¹H, ¹³C and ¹⁹F NMR spectroscopies, mass spectrometry, IR spectroscopy and microanalysis. The molecular structures of four compounds (**4a/b**, **6a** and **7**) were further confirmed by X-ray crystallography. The biological activities of the organometallic-intermediates (**4a/b**) and organometallic-derivatives of monepantel (**5a/b**, **6a/b** and **7**) were evaluated *in vitro* using parasitic nematodes of major importance in livestock, namely *Haemonchus contortus* and *Trichostrongylus colubriformis*. Two ferrocenyl compounds (**4a** and **6a**) showed nematocidal activity, while the analogous ruthenocenyl compounds (**4b** and **6b**) were not active at the highest concentration tested (10 µg/mL). In order to obtain insight into the difference in activity of ferrocenyl and ruthenocenyl derivatives, the potential of the compounds for reactive oxidative species (ROS) production in living cells was assessed. Interestingly, neither the ferrocenyl nor the ruthenocenyl compounds (**4a/b** and **6a/b**) produced significant ROS in HeLa cells, indicating a redox-independent activity of **4a** and **6a** on parasites. The selectivity of the compounds towards parasites was further confirmed through the investigation of the cytotoxic profile of all the compounds. All of them were found to be non-toxic either to HeLa or to MRC-5 cell lines. Thus, **4a** and **6a** could be considered as interesting leads for further development of new classes of anti-parasitic agents.

Introduction

The impact of parasitic diseases on animals and humans is substantial around the world. Controlling parasites of domesticated animals is a major issue, and usually relies exclusively on chemotherapy with an arsenal of broad-spectrum anthelmintics.^{3,4} The excessive use of these drugs has resulted in the emergence of resistance, and multi-drug resistance is now widespread.⁶⁻⁹ Apart from the three classical groups of anthelmintics, i.e. the benzimidazoles, imidazothiazoles and macrocyclic lactones, a new synthetic anthelmintic class, the amino-acetonitrile derivatives (AADs, see Scheme 1), has been discovered, and a promising candidate of this class, called monepantel, was recently commercialized.^{1,10,11}

Investigations have unveiled that the safety profile of monepantel relates to its target, a nematode specific nicotinic acetylcholine receptor (nAChR) subunit, which is absent from host mammals.¹²⁻¹⁴ Although monepantel now represents a new class of anthelmintic drug, unfortunately, few years after its introduction and use in the field, nematodes with reduced sensitivity to monepantel have already been detected in countries including Uruguay, New Zealand and Brazil.¹⁵⁻¹⁹ Given this rapid emergence of resistance to monepantel, there is an urgent need to develop novel and improved control strategies to ensure the sustainability of parasite control. With this in mind, our group has recently started to derivatize monepantel with various organometallic moieties using different strategies (Scheme 1).^{20,21} The derivatization of a known organic drug with organometallic moieties has proven to be extremely successful in various fields of medicinal chemistry.²²⁻³⁶

Ferroquine, a ferrocenyl analogue of the antimalarial drug chloroquine, is one of the best examples of such a derivatization. Different metal-specific mode of actions made ferroquine active against chloroquine-resistant strains of the malaria parasite, *Plasmodium falciparum* (*P. falciparum*).^{30,37,38} In our initial study, we replaced the aryloxy unit of monepantel with organometallic moieties and modified the benzamide part with various functional groups (Scheme 1, Strategy I/II).²⁰ Subsequently, we replaced the chiral C2 spacer of monepantel by a ferrocenyl moiety that comprised planar chirality with a 1,2-unsymmetric substitution cyclopentadienyl ring (Scheme 1, Strategy III).²¹



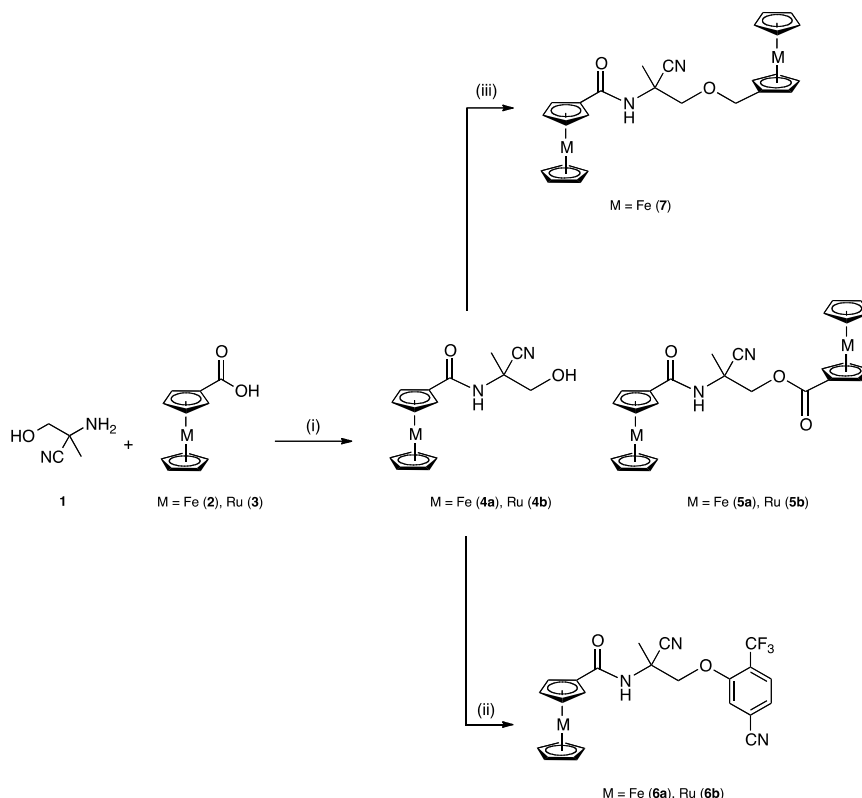
Scheme 1. Schematic representation of previous (green) and new (red) designed organometallic derivatives of monopantel (AAD 1566) using different strategies. OM = ferrocene, ruthenocene or cymantrene; FG = SCF₃, F, Cl, Br, I, SCH₃, CF₃, OCF₃, S(O)CF₃, S(O)₂CF₃.

Extending this work to develop organometallic monopantel derivatives, we report here a new strategy for achieving structurally distinct organometallic-containing monopantel derivatives. First, we kept the aryloxy unit of monopantel unperturbed and substituted the benzamide unit with metallocenes, namely ferrocene and ruthenocene (Scheme 1, Strategy IV). Then, we replaced simultaneously both the aryloxy and the benzamide units using two metallocenyl fragments (Scheme 1, Strategy IV). During the course of the present study, we prepared ferrocenyl monopantel derivatives, since the presence of the ferrocenyl unit might result in additional metal-specific modes of action, such as the production of ROS under physiological conditions. In order to investigate if these redox reactions contribute to the antiparasitic activity of our novel organometallic compounds, we designed ruthenocenyl analogous of the ferrocenyl monopantel derivatives. The replacement of the iron(II) in the derivatives by a ruthenium(II) center should prevent redox reactions under physiological relevant conditions responsible for ROS production.^{37,38}

Results and Discussion

Synthesis and Characterization

The ferrocenyl and ruthenocenyl analogues of monepantel corresponding to Strategy IV were prepared in a two-step reaction procedure as presented in Scheme 2. In order to obtain initial insights into their potential as anthelmintic agents, we focused on the isolation of the organometallic derivatives as racemates rather than as enantiomerically pure compounds.



Scheme 2. Reagents and conditions: (i) a) oxalyl chloride, dry CH_2Cl_2 , r.t.; b) NEt_3 , dry THF, r.t., o.n., **4a** (50%), **4b** (31%), **5a** (11%), **5b** (19%); (ii) NaH, 3-fluoro-4-(trifluoromethyl)benzonitrile, dry THF, overnight, $0^\circ\text{C} \rightarrow \text{r.t.}$, **6a** (26%) **6b** (11%); (iii) (ferrocenylmethyl)trimethylammonium iodide, K_2CO_3 , 18-crown-6, dry CH_3CN , reflux, o.n., **7** (43%).

The syntheses of desired organometallic analogues commenced with the preparation of a 2-amino-2-hydroxymethylpropanenitrile (**1**) synthon, following a literature procedure by Gauvry *et al.*³⁹ The intermediate *N*-(2-cyano-1-hydroxypropan-2-yl)ferroceneamide (**4a**) was obtained in a moderate amount after reacting activated ferrocenecarboxylic acid (**2**) with **1** under basic conditions. Moreover, the same reaction allowed the isolation of the first di-ferrocenyl analogue of monepantel, 2-ferroceneamido-2-cyanopropyl ferroceneoate (**5a**), with an 11% yield. Compound **4a**

was converted to the final product *N*-(2-cyano-1-(5-cyano-2-(trifluoromethyl)phenoxy)propan-2-yl)ferroceneamide (**6a**), yielding 26% using a Williamson ether synthesis in the presence of NaH and of the commercially available 3-fluoro-4-(trifluoromethyl)benzotrile. In addition to the first di-ferrocenyl analogue **5a**, another disubstituted organometallic analogue, namely *N*-(1-(ferrocenyloxy)-2-cyanopropan-2-yl)ferroceneamide (**7**) was also prepared by reacting **4a** with (ferrocenylmethyl)trimethylammonium iodide under basic conditions. By contrast to **5a**, where one of the ferrocenyl units is linked to C2 spacer by an ester bond, the similar ferrocene unit in **7** is attached to the C2 spacer by an ether bond. Moreover, we synthesized three ruthenocenyl analogues (**4b**, **5b** and **6b**), which are structurally identical to the ferrocenyl analogues **4a**, **5a** and **6a**. As ferrocene and ruthenocene are iso-structural but have distinct redox properties, comparison of the biological activity of ferrocenyl and the corresponding ruthenocenyl analogues might shed light on the possible involvement of the redox properties in their activity. The synthetic sequences to obtain the desired ruthenocenyl analogues of monepantel are similar to those of ferrocenyl compounds (see Scheme 2). All novel ferrocenyl and ruthenocenyl analogues of monepantel described here were isolated as racemic mixtures and characterized by ¹H, ¹³C, ¹⁹F NMR spectroscopies, ESI-mass spectrometry (positive detection mode) and IR spectroscopy, and their purities were analyzed by microanalysis.

X-ray Crystallography.

X-ray crystallography further confirmed the molecular structures of four compounds (**4a/b**, **6a** and **7**). Details on how the compound were crystallized can be found in the experimental section. The amide unit is coplanar with the cyclopentadienyl ring. The alcohol of compound **4a** is part of a cyclic and a linear hydrogen-bridge network. The R₂²(14) cycle⁴⁰ is formed by an alcohol hydrogen, making contact with a symmetry (-x, 1-y, -z)-related carbonyl oxygen; the corresponding alcohol donates back to the original carbonyl oxygen. Additionally, the same alcohol is an acceptor of a hydrogen bridge from a symmetry related amide nitrogen (-x, 1/2+y, 1/2-z). The structures of **4a** and **4b** are essentially isostructural, with the major difference being that the Fe-C bond lengths in **4a** are between 2.0293(14) Å and 2.0619(17) Å, whereas the Ru-C bond lengths in **4b** are between 2.155(3) Å and 2.192(3) Å (see Figure 1). Compound

6a does not form any "typical" hydrogen bonds, despite the presence of an amide unit (see Figure 1).

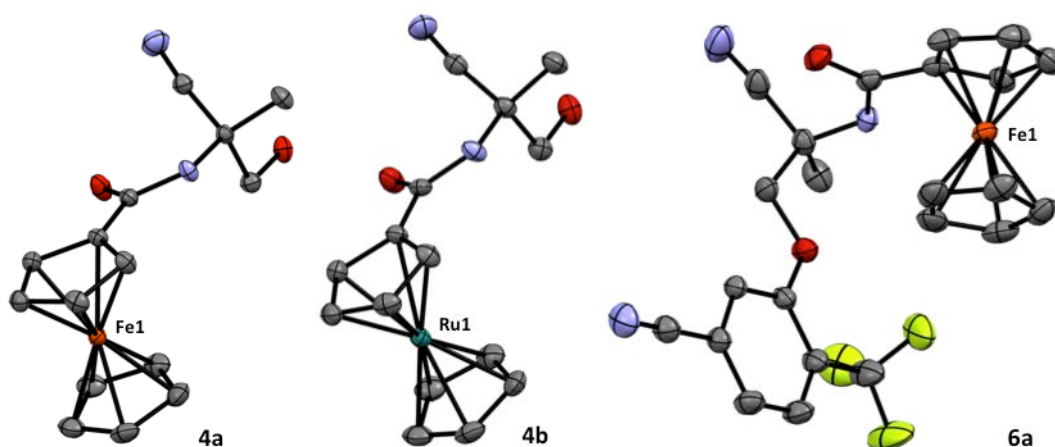


Figure 1. Molecular structures of **4a**, **4b** and **6a** with atoms shown as thermal ellipsoids (drawn at 50% probability; hydrogen atoms are omitted for clarity).

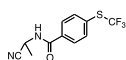
Compound **7** was measured on a synchrotron; it crystallized with two molecules in the asymmetric unit. All cyclopentadienyl rings of the 4 ferrocene units are in an almost perfect eclipsed conformation. One linker starting from the quaternary carbon to the methylene unit next to the cyclopentadienyl ring is disordered in a ratio 3:2 (see SI for structure).

Biological Evaluation

The anthelmintic potentials of our ferrocenyl and ruthenoceryl precursors (**4a/b**) and final derivatives **5a/b**, **6a/b** and **7** were evaluated on two common parasites of small ruminants, *Haemonchus contortus* (*H. contortus*) and *Trichostrongylus colubriformis* (*T. colubriformis*) using a larval development assay (LDA) (see Experimental Section for details). The results are summarized in Table 1. The organic derivatives AAD85 and AAD96 were included as controls.¹

Table 1. Antiparasitic activity of **4a/b**, **5a/b**, **6a/b**, **7** against *Haemonchus contortus*, *Trichostrongylus colubriformis* and *Dirofilaria immitis* and cytotoxicity against HeLa and MRC-5 cells (^a EC₁₀₀ value¹; ^b taken from the literature²; n.d.i. = non-disclosable information⁵ and n.d. = not determined).

<i>H. contortus</i>	<i>T. colubriformis</i>	<i>D.immitis</i> 24 hours
---------------------	-------------------------	------------------------------



Two of seven metal-based monepantel derivatives tested displayed moderate activities against *H. contortus* and *T. colubriformis*. The final ferrocenyl derivative of Strategy IV (**6a**) and its corresponding ferrocene precursor (**4a**) showed EC₆₀ values in a similar range when tested against *H. contortus* 4.90 µg/mL (**4a**) and 4.70 µg/mL (**6a**) and *T. colubriformis* 8.00 µg/mL (**4a**) and 7.00 µg/mL (**6a**). Interestingly, the potency of both active derivatives (**4a**, **6a**) is twice as high against *H. contortus* compared with *T. colubriformis*. However, the potencies of **4a** and **6a** are lower when compared with the organic controls AAD85 and AAD96, which displayed EC₁₀₀ values of 0.032 µg/mL and 0.01 µg/mL against *H. contortus* and *T. colubriformis*, respectively.¹ Importantly, the ruthenocenyl analogues (**4b**, **5b**) of the active ferrocenyl derivatives **4a**, **5a** displayed no activity against *H. contortus* and *T. colubriformis* at the highest concentration evaluated (10 µg/mL). At this point, it is reasonable to speculate that

the iron(II) centre in **4a** and **6a** contributes to the production of toxic ROS, leading to the anti-parasitic activity. Therefore, we evaluated ROS generation using the ferrocene and ruthenocene-containing derivatives in live cells (Figure 1). Although an assessment of ROS generation in the parasitic nematodes would have been ideal, for technical reasons this was not possible, such that we elected to use a mammalian cervical cancer cell line (HeLa) as model. The ROS production in the cells treated with **4a/b** and **6a/b** (25 μ M for 22 h) was quantified using the fluorescent indicator 2',7'-dichlorofluorescein diacetate (H₂DCFDA). As positive control, *tert*-butyl hydroperoxide (TBH) was included in same assay. We have already shown that Zolvix[®] does not produce ROS.²⁰ Surprisingly, the ROS levels in cells treated with the ferrocenyl compounds (**4a**, **6a**) and the ruthenocetyl compounds (**4b**, **6b**) did not display a significant difference, being comparable to the ROS level of untreated cells (Figure 1).²⁰

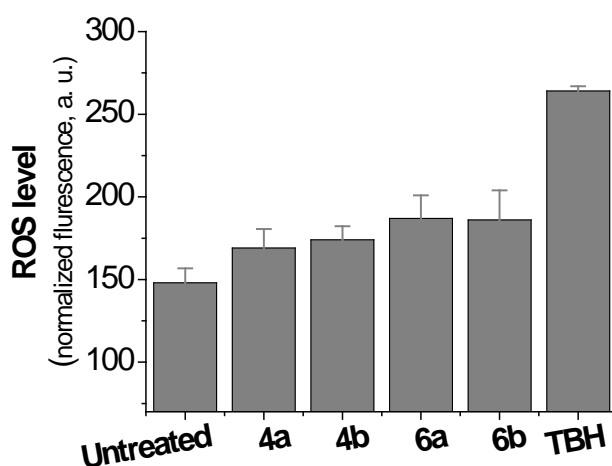


Figure 1. Level of ROS production in HeLa cells untreated or treated with **4a**, **4b**, **6a** and **6b**. TBH = *tert*-butyl hydroperoxide.

Hence, the results suggest that the differences in anti-parasitic activity between the ferrocene- and ruthenocene-containing organometallic compounds are not related to the production of ROS in cells. The potency of the organometallic monepantel derivatives synthesized using Strategy IV against *H. contortus* and *T. colubriformis* is lower than for the organometallic derivatives from Strategy I/II, but superior to those from Strategy III.^{20,21} Overall, based on knowledge obtained from these structure-activity relationships of organometallic monepantel derivatives, it can be concluded that it is preferable to keep the benzamide part of monepantel unperturbed, while

structural modifications can be made to the aryloxy portion for the designing of new derivatives of monepantel with anti-parasitic activity against *H. contortus* and *T. colubriformis*. Previous studies have shown that organometallic derivatization can modify the spectrum of activity of a known organic drug through the addition of metal-specific mode of actions.^{38,41} Therefore, we decided to evaluate the present compounds further against other parasites.^{42,43} The activity of our organometallic-analogues of monepantel was evaluated on the canine heartworm, *Dirofilaria immitis* (*D. immitis*). Two ruthenocenyl compounds (**5b**, **6b**) showed moderate activity against microfilariae of this nematode species in a 48 h motility assay with EC₅₀ values of 6.60 µg/mL. Interestingly, the corresponding ferrocenyl derivatives **5a** and **6a** are inactive against *D. immitis*. However, once again, **5b** and **6b** are less potent compared to the organic control AAD85, which displays an EC₅₀ value of 2.20 µg/mL.⁵ We also investigated the activity of the ferrocenyl and ruthenocenyl precursors (**4a/b**) and final derivatives **5a/b**, **6a/b** and **7** on three arthropods *C. felis* (cat flea), *L. cuprina* (blow fly) and *R. sanguineus* (brown dog tick). Unfortunately, none of the compounds synthesized displayed potency at the highest concentration tested on *C. felis* (100 µg/mL), *L. cuprina* (32 µg/mL) or *R. sanguineus* (100 µg/mL and 640 µg/mL) (Table S1).

For development of new anti-parasitic compounds, the selectivity of the compounds towards parasites is an important parameter to consider. An ideal anthelmintic should be non-toxic to the host, while being efficient in killing worms. For this purpose, we evaluated the cytotoxicity of the compounds on a cervical cancer cell line (HeLa) and a non-cancerous human lung fibroblast cell line (MRC-5). None of the compounds tested were toxic up to 100 µM (the highest concentration assayed), indicating selectivity of our compounds (**4a**, **6a**) to the nematodes *H. contortus*, *T. colubriformis* and *D. immitis* over mammalian cells.

Conclusion

The extensive use of commercially available broad-spectrum organic anthelmintics has led to a situation where parasites are resistant to at least one or more available drug classes. With the view of developing a new class of metal-based anthelmintic agents, we present here a study where we replaced either the benzamide unit of monepantel with a metallocenyl fragment or coupled two metallocenyl units to the C2 spacer of the same original drug. The biological efficacy of the all ferrocene- and ruthenocene-containing derivatives (**4a/b**, **5a/b**, **6a/b**, **7**) was assessed in a LDA against *H. contortus* and *T. colubriformis*. Two ferrocenyl derivatives **4a** and **6a** showed moderate efficacy with EC₆₀ values between 4.70 – 8.00 µg/mL against both nematode species, while the corresponding ruthenocenyl derivatives displayed no activity. The ROS production of both types of organometallic derivatives (**4a/b** and **6a/b**) was evaluated in an *in vitro* model using the HeLa cancerous cervical cell line. However, no significant difference in ROS levels was observed between the ferrocenyl (**4a** and **6a**) and ruthenocenyl (**4b** and **6b**) analogues. This unexpected finding might suggest a redox independent mode of action for the anti-parasitic activity of the ferrocenyl derivatives (**4a** and **6a**). The selectivity of the compounds towards parasites was demonstrated by assessment of their cytotoxicity using a cancerous (HeLa) and a non-cancerous (MRC-5) cell line.

Experimental Section

Materials

All chemicals were of reagent grade quality or better, obtained from commercial suppliers and used without further purification. Solvents were used as received or distilled using standard procedures.⁴⁴ All preparations were carried out using standard Schlenk techniques. *Thin layer chromatography (TLC)* was performed using silica gel 60 F-254 (Merck) plates with detection of spots being achieved by exposure to UV light. *Column chromatography* was performed using Silica gel 60 (0.040-0.063 mm mesh, Merck). Eluent mixtures are expressed as volume to volume (v/v) ratios. Chlorocarbonyl ferrocene and chlorocarbonyl ruthenocene were synthesized according to literature procedures.⁴⁵

Instrumentation and Methods

¹H, ¹³C and ¹⁹F NMR spectra were recorded in deuterated solvents on Bruker AV2-401, AV2-400, AV-500 and AV-501 at room temperature. The chemical shifts, δ , are reported in ppm (parts per million). The signals from the residual protons of deuterated solvent have been used as an internal reference.^{46,47} The abbreviations for the peak multiplicities are as follows: s (singlet), d (doublet), dd (doublet of doublets), t (triplet), q (quartet), m (multiplet), and br (broad). *ESI mass spectrometry* was performed using a Bruker Esquire 6000 spectrometer. In the assignment of the mass spectra, the most intense peak is listed. UPLC-ESI-MS was performed on a Waters Acquity UPLC System coupled to a Bruker HCTTM, using an Acquity UPLC BEH C18 1.7 μ m (2.1 x 50 mm) as a reverse phase column with a flow rate of 0.6 mL min⁻¹. The UV absorption was measured at 254 nm. The runs were performed with a linear gradient of A (acetonitrile (Sigma-Aldrich HPLC grade) and B (distilled water containing 0.02% TFA and 0.05% HCOOC): t = 0 – 0.5 min, 5% A; t = 4.0 min, 100% A; t = 5 min, 100% A. *High-resolution mass spectrometry* were performed on a Bruker ESQUIRE-LC quadrupole ion trap instrument (Bruker Daltonik GmbH, Bremen, Germany), equipped with a combined Hewlett-Packard Atmospheric Pressure Ion (API) source (Hewlett-Packard Co., Palo Alto, CA, USA). The solutions (about 0.1-1 μ mol/ml) were continuously introduced through the electrospray interface with a syringe infusion pump (Cole-Parmer 74900-05, Cole-Parmer Instrument Company, Vernon Hills, Illinois, USA) at a flow rate of 5 μ l min⁻¹. The MS-conditions were: Nebulizer

gas (N₂) 15 psi, dry gas (N₂) 7 min⁻¹, dry temperature 300°C, capillary voltage 4000 V, end plate 3500 V, capillary exit 100 V, skimmer1 30 V, and trap drive 70. The MS acquisitions were performed at normal resolution (0.6 u at half peak height), under ion charge control (ICC) conditions (10'000) in the mass range from m/z 100 to 2000. To get representative mass spectra, 8 scans were averaged. *Infrared spectra* were recorded on Perkin-Elmer FTIR spectrometer using KBr pellets. Peak intensities are given as broad (b), very strong (vs), strong (s), medium (m) and weak (w). *Elemental microanalyses* were performed on a LecoCHNS-932 elemental analyser.

Synthesis

N-(2-cyano-1-hydroxypropan-2-yl)ferroceneamide (**4a**) and 2-Ferroceneamido-2-cyanopropyl ferroceneoate (**5a**).

Chlorocarbonyl ferrocene (0.648 g, 2.608 mmol) and 2-amino-2-hydroxymethylproprionitrile (0.261 g, 2.608 mmol) were dissolved in dry THF (100 mL). To this orange reaction solution NEt₃ (453 μL, 3.26 mmol) was added and the mixture was stirred overnight at room temperature. The solvent was evaporated under reduced pressure. The crude residue was redissolved in CH₂Cl₂ (30 mL), washed with H₂O (2 x 10 mL) and brine (2 x 10 mL). The organic layer was dried with MgSO₄, filtered and the solvent was evaporated under reduced pressure. The crude product was purified by column chromatography on silica with hexane:ethyl acetate (4:1) as the eluent (R_f (**5a**) = 0.69, hexane:ethyl acetate (1:1), R_f (**4a**) = 0.30, hexane:ethyl acetate (1:1)) to afford 2-ferroceneamido-2-cyanopropyl ferroceneoate (**5a**) and *N*-(2-cyano-1-hydroxypropan-2-yl)ferroceneamide (**4a**) as orange solids, respectively. Yield: 11% (**5a**, 0.075 g, 0.143 mmol) and 50% (**4a**, 0.41 g, 1.31 mmol). Data **4a**: IR (KBr, cm⁻¹): 3467_s, 3412_s, 3103_w, 2941_w, 2862_w, 1635_s, 1534_m, 1454_w, 1377_w, 1312_m, 1267_w, 1201_w, 1160_w, 1099_w, 1056_m, 1037_w, 1023_w, 998_w, 911_w, 826_w, 772_w, 710_w, 620_m, 528_w, 499_w, 483_w, 464_w. ¹H NMR (400 MHz, d⁶-acetone): δ/ppm = 7.12 (s, 1H, NH), 5.01 (t, ³J = 6.4 Hz, 1H, OH), 4.85-4.84 (m, 2H, C₅H₄), 4.39-4.38 (m, 2H, C₅H₄), 4.24 (s, 5H, C₅H₅), 4.0-3.93 (m, 1H, CH₂), 3.90-3.86 (m, 1H, CH₂), 1.71 (s, 3H, CH₃). ¹³C NMR (125 MHz, d⁶-acetone): δ/ppm = 170.9, 121.1, 76.1, 71.5, 70.5, 69.5, 69.4, 67.0, 66.9, 53.3, 22.6. ESI-MS: m/z (%) = 351.02 [M+K]⁺ (8), 335.04 [M+Na]⁺ (100), 312.06 [M]⁺ (52). HR ESI-MS: m/z (%) = 312.05557, calcd. for C₁₅H₁₆FeN₂O₂ (M⁺) m/z (%) = 312.05508. Elemental analysis: calcd. for

$C_{15}H_{16}N_2O_2Fe = C, 57.72; H, 5.17; N, 8.97$. Found = $C, 57.48; H, 5.13; N, 8.69$. Data **5a**: IR (Golden Gate, cm^{-1}): 3368w, 1690m, 1656m, 1520m, 1453w, 1378w, 1288m, 1264w, 1214w, 1164m, 1144m, 1104w, 1027w, 999w, 918w, 827m, 814m, 770m, 741w. 1H NMR (500 MHz, d^6 -acetone): $\delta/ppm = 7.53$ (s, 1H, NH), 4.88-4.87 (m, 4H, C_5H_4), 4.77 (d, $^2J = 10.8$ Hz, 1H, CH_2), 4.82-4.50 (m, 3H, C_5H_4, CH_2), 4.44-4.41 (m, 2H, C_5H_4), 4.27 (s, 5H, C_5H_5), 4.25 (s, 5H, C_5H_5), 1.90 (s, 3H, CH_3). ^{13}C NMR (125 MHz, d^6 -acetone): $\delta/ppm = 171.7, 170.7, 120.21, 75.8, 72.7, 71.7, 71.0, 70.8, 70.6, 69.5, 69.4, 66.9, 51.5, 23.1$. ESI-MS: m/z (%) = 524.1 $[M]^+$ (100). Elemental analysis: calcd. for $C_{26}H_{24}N_2O_3Fe_2 = C, 59.58; H, 4.62; N, 5.34$. Found = $C, 59.51; H, 4.52; N, 5.25$.

N-(2-cyano-1-hydroxypropan-2-yl)ruthenoceneamide (**4b**) and 2-cyano-2-(ruthenocenecarboxamido)propyl ruthenocnecarboxylate (**5b**).

Chlorocarbonyl ruthenocene (1.67 g, 6.96 mmol) and 2-amino-2-hydroxymethylproprionitrile (1.05 g, 10.5 mmol) were dissolved in dry THF (50 mL). To this colourless reaction solution NEt_3 (6.8 mL, 50 mmol) was added and the mixture was stirred overnight at room temperature. The solvent was evaporated under reduced pressure. The crude product was purified by column chromatography on silica with hexane:ethyl acetate (7:1 \rightarrow 1:7) and methanol as the eluent (R_f (**4b**) = 0.05, hexane:ethyl acetate (7:1), R_f (**5b**) = 0.2, methanol) to afford *N*-(2-cyano-1-hydroxypropan-2-yl)ruthenocenamide (**4b**) and 2-cyano-2-(ruthenocenecarboxamido)propyl ruthenocnecarboxylate (**5b**) as pale yellow solids, respectively. Yield: 31% (**4b**, 0.77 g, 2.06 mmol) and 19% (**5b**, 0.81 g, 1.32 mmol). Data **4b**: IR (KBr, cm^{-1}): 3248br, 31122s, 3056w, 2943w, 2887w, 2641w, 2324w, 2241w, 2050w, 1981w, 1720w, 1633s, 1531s, 1455s, 1376s, 1308s, 1130s, 823s. 1H NMR (500 MHz, DMSO): $\delta/ppm = 7.51$ (s, 1H, NH), 5.64 (t, $^3J = 6.46$ Hz, 1H, OH), 5.23-5.22 (m, 2H, C_5H_4), 4.73-4.73 (m, 2H, C_5H_4), 4.59 (s, 5H, C_5H_5), 3.80-3.76 (m, 1H, CH_2), 3.53-.3.50 (m, CH_2), 1.54 (s, 3H, CH_3). ^{13}C NMR (125 MHz, DMSO): $\delta/ppm = 168.1, 120.5, 79.1, 72.4, 72.3, 71.6, 70.4, 70.3, 64.8, 51.9, 21.7$. ESI-MS: m/z (%) = 359.1 $[M+H]^+$ (100), 259.0 $[M-C_4H_4N_2OH]^+$ (17). Elemental Analysis: calcd. for $C_{15}H_{16}O_2N_2Ru = C, 50.41; H, 4.51; N, 7.84$. Found = $C, 50.85; H, 4.44; N, 7.41$. Data **5b**: IR (KBr, cm^{-1}): 3320m, 3104w, 2956w, 2651w, 2322w, 2161s, 2053s, 1976s, 1690s, 1656s, 1521s, 1450s, 1373s, 1267s, 1135s, 1035m, 997m, 808s, 759m. 1H

NMR (500 MHz, DMSO): δ /ppm = 7.93 (s, 1H, NH), 5.27-5.25 (m, 2H, C₅H₃), 5.15-5.13 (m, 2H, C₅H₃), 4.85-4.84 (m, 2H, C₅H₄), 4.76-4.75 (m, 2H, C₅H₄), 4.65 (s, 5H, C₅H₃), 4.59 (s, 5H, C₅H₃), 4.51 (d, ²J = 10.8, 2H, CH₂), 4.27 (d, ²J = 10.4, 2H, CH₂), 1.66 (s, 3H, CH₃). ¹³C NMR (125 MHz, DMSO): δ /ppm = 168.6, 168.2, 119.2, 78.7, 74.1, 73.3, 72.5, 71.9, 71.6, 71.4, 70.5, 70.3, 64.9, 49.7, 22.1. ESI-MS: m/z (%) = 639.3 [M+Na]⁺ (100). Elemental analysis: calcd. for C₂₆H₂₄O₃N₂Ru₂ = C, 50.81; H, 3.94; N, 4.56. Found = C, 50.92; H, 3.96; N, 4.53.

N-(2-cyano-1-(5-cyano-2-(trifluoromethyl)phenoxy)propan-2-yl)ferroceneamide (**6a**)

N-(2-cyano-1-hydroxypropan-2-yl)ferroceneamide (**4a**, 0.020 g, 0.064 mmol) was dissolved in dry THF (30 mL). The orange solution was cooled to 0°C and NaH (1.8 mg, 0.074 mmol) was added. After stirring the reaction mixture for 30 min at 0°C 3-fluoro-4-(trifluoromethyl)benzotrile (0.012 g, 0.064 mmol) was. After stirring the reaction mixture overnight at room temperature, additional NaH (1.8 mg, 0.074 mmol) and 3-fluoro-4-(trifluoromethyl)benzotrile (0.012 g, 0.064 mmol) were added to the reaction mixture. Another portion of NaH (1.8 mg, 0.074 mmol) was added 2 h later. The reaction was quenched with H₂O (2 mL) and brine (6 mL) and the aqueous layer was extracted with ethyl acetate (3 x 10 mL). The combined organic layers were dried over MgSO₄, filtered and the solvent was evaporated under reduced pressure. The crude product was purified by column chromatography on silica with hexane:ethyl acetate (6:1) as the eluent (R_f = 0.36, hexane:ethyl acetate (2:1)) to give *N*-(2-cyano-1-(5-cyano-2-(trifluoromethyl)phenoxy)propan-2-yl)ferroceneamide (**6a**) as an orange solid. Yield: 26% (0.041 g, 0.085 mmol). IR (KBr, cm⁻¹): 3478s, 3414s, 3355s, 2925s, 2851m, 2358m, 2336m, 2240s, 1653s, 1613s, 1574w, 1527m, 1510w, 1465m, 1415m, 1409w, 1373w, 1309m, 1281m, 1261w, 1211w, 1180m, 1141m, 1131m, 1037m, 895w, 841w, 822w, 632w, 606w, 531w, 503w, 486w. ¹H NMR (400 MHz, d⁶-acetone): δ /ppm = 7.90 (d, ³J = 8.4 Hz, 1H, arom.), 7.84 (s, 1H, arom.), 7.61 (d, ³J = 7.6 Hz, 1H, arom.), 7.52 (s, 1H, NH), 4.88-4.83 (m, 2H, C₅H₄; 1H, CH₂), 4.67 (d, ²J = 9.2 Hz, 1H, CH₂), 4.41-4.40 (m, 2H, C₅H₄), 4.22 (s, 5H, C₅H₅), 1.93 (s, 3H, CH₃). ¹³C NMR (125 MHz, d⁶-acetone): δ /ppm = 170.9, 157.0, 129.3, 129.2, 129.2, 129.1, 126.0, 125.1, 123.2, 123.0, 122.9, 119.7, 118.4, 118.0, 75.6, 71.9, 71.7, 71.6, 70.6, 69.6, 69.4, 51.2, 23.0. ¹⁹F NMR (282.23 MHz, d⁶-acetone): δ /ppm = -63.6. ESI-MS: m/z (%) = 504.0 [M+Na]⁺ (100), 985.1 [2M+Na]⁺ (12). HR ESI-MS: m/z (%) =

504.05927 calcd. for $C_{23}H_{18}F_3FeN_3NaO_2$ ($[M+Na]^+$) m/z (%) = 504.05958. Elemental analysis: calcd. for $C_{23}H_{18}N_3O_2F_3Fe$ = C, 57.40; H, 3.77; N, 8.73. Found = C, 57.62; H, 4.01; N, 8.38.

N-(2-cyano-1-(5-cyano-2-(trifluoromethyl)phenoxy)propan-2-yl)ruthenoceneamide (**6b**)

N-(2-cyano-1-hydroxypropan-2-yl)ruthenocenamide (**4b**, 150 mg, 0.42 mmol) was dissolved in dry THF (30 mL). The colorless solution was cooled to 0°C and NaH (15 mg, 0.63 mmol) was added. After stirring the reaction mixture for 30 min at 0°C 3-fluoro-4-(trifluoromethyl)benzotrile (80 mg, 0.42 mmol) was. After stirring the reaction mixture overnight at room temperature, additional NaH (5 mg, 0.21 mmol) and 3-fluoro-4-(trifluoromethyl)benzotrile (40 mg, 0.21 mmol) were added to the reaction mixture and the reaction was allowed to stir for another 3 h. The reaction was quenched with H₂O (2 mL) and brine (6 mL) and the aqueous layer was extracted with ethyl acetate (3 x 10 mL). The combined organic layers were dried over Na₂SO₄, filtered and the solvent was evaporated under reduced pressure. The crude product was purified by column chromatography on silica with hexane:ethyl acetate (2:1) as the eluent (R_f = 0.60,) to give *N*-(2-cyano-1-(5-cyano-2-(trifluoromethyl)phenoxy)propan-2-yl)ruthenoceneamide (**6b**) as an colorless solid. Yield: 11% (0.024 g, 0.046 mmol). IR (KBr, cm^{-1}): 3341 br , 3076 br , 2952 w , 2234 s , 2165 w , 1977 s , 1630 s , 1575 s , 1528 s , 1416 s , 1285 s , 1264 s , 1186 s , 1132 s , 1039 s , 816 s , 815 s , 735 s . ¹H NMR (500 MHz, d^6 -acetone): δ/ppm = 7.89 (d, ³ J = 8.0 Hz, 1H, arom. H), 7.80 (s, 1H, arom. H), 7.61 (d, ³ J = 8.0 Hz, 1H, arom. H), 7.34 (s, 1H, NH), 5.20-5.19 (m, 2H, C_5H_4), 4.77 (d, ³ J = 9.5 Hz, 1H, CH_2), 4.71 (s, 2H, C_5H_4), 4.60-4.58 (m, 6H, CH_2 and C_5H_5), 1.87 (s, 3H, CH_3). ¹³C NMR (125 MHz, d^6 -acetone): δ/ppm = 169.6, 169.5, 157.0, 156.9, 129.3, 129.3, 129.2, 129.2, 127.2, 126.1, 125.1, 123.5, 123.3, 123.0, 122.9, 122.8, 120.7, 119.6, 118.4, 118.4, 118.1, 118.0, 79.9, 79.9, 73.2, 73.2, 72.5, 72.0, 72.0, 71.2, 71.1, 51.2, 51.1, 22.9, 22.9. ¹⁹F NMR (470.59 MHz, d^6 -acetone): δ/ppm = -63.4. ESI-MS: m/z (%) = 550.0 $[M+Na]^+$ (100). HR ESI-MS: m/z = 528.04751, calcd. for $C_{23}H_{18}F_3N_3O_2Ru$ ($[M]$) m/z = 528.04733; m/z (%) = 550.02942, calcd. for $C_{23}H_{18}F_3N_3NaO_2Ru$ ($[M+Na]$) m/z (%) = 550.02928. Elemental analysis: calcd. for $C_{23}H_{21}F_3N_3O_3Ru$ = C. 52.47; H, 3.45; N, 7.98. Found = C. 50.61; H, 3.40; N, 7.51.

N-(1-(ferrocenyloxy)-2-cyanopropan-2-yl)ferroceneamide (**7**)

N-(2-cyano-1-hydroxypropan-2-yl)ferroceneamide (**4a**, 0.03 g, 0.096 mmol), (ferrocenylmethyl)trimethylammonium iodide (0.065 g, 0.17 mmol), K₂CO₃ (39.8 mg, 0.288 mmol) and 18-crown-6 (7.6 mg, 0.0288 mmol) were dissolved in dry CH₃CN (20 mL) and refluxed (90°C) for 120 h. Additional (ferrocenylmethyl)trimethylammonium iodide (0.065 g, 0.17 mmol) was added to the reaction and further refluxed overnight. The orange reaction mixture was allowed to reach room temperature. The solvent was evaporated under reduced pressure. The crude residue was redissolved in Et₂O (10 mL) and washed with H₂O (2 x 5 mL) and brine (2 x 5 mL). The organic phase was dried over MgSO₄, filtered and the solvent was evaporated under reduced pressure. The crude product was purified by column chromatography on silica using hexane:ethyl acetate (3:1) as the eluent (R_f = 0.29) to afford *N*-(1-(ferrocenyloxy)-2-cyanopropan-2-yl)ferroceneamide (**7**) as a yellow solid. Yield: 43% (0.021 g, 0.041 mmol). IR (KBr, cm⁻¹): 3469_s, 2929_w, 2852_w, 1637_s, 1518_s, 1378_w, 1339_w, 1305_w, 1280_w, 1101_m, 1008_m, 825_m, 523_m, 502_m, 485_m. ¹H NMR (500 MHz, CD₃CN): δ/ppm = 6.48 (s, 1H, NH), 4.73-4.70 (m, 2H, C₅H₄), 4.46 (s, 2H, RCH₂OR), 4.39-4.38 (m, 2H, C₅H₄), 4.32-4.31 (m, 2H, C₅H₄), 4.20 (s, 7H, C₅H₅, C₅H₄), 4.17 (s, 5H, C₅H₅), 3.80 (d, ³J = 9.3 Hz, 1H, CH₂), 3.70 (d, ³J = 9.3 Hz, 1H, CH₂), 1.68 (s, 3H, CH₃). ¹³C NMR (125 MHz, CD₃CN): δ/ppm = 207.9, 171.2, 121.2, 83.9, 75.6, 73.5, 71.9, 70.7, 70.6, 70.5, 69.6, 69.5, 69.5, 69.4, 51.7, 22.9. ESI-MS: *m/z* (%) = 484.03 [M-CN]⁺ (12), 510.04 [M]⁺ (100), 533.00 [M+Na]⁺ (7). HR ESI-MS: *m/z* (%) = 510.06882, calcd. for C₂₆H₂₆Fe₂N₂O₂ ([M+Na]⁺) *m/z* (%) = 510.06864. Elemental analysis: calcd. for C₂₆H₂₆N₂O₂Fe₂ = C, 61.21; H, 5.14; N, 5.49. Found = C, 61.06; H, 5.20; N, 5.31.

Crystallographic Studies

Single crystals of **4a** and **7** were grown after slow evaporation of an acetonitrile solution containing **4a** or **7** respectively. Single crystals of **4b** were grown after slow evaporation of an dichloromethane solution containing **4b**. Single crystals of **6a** were grown after slow evaporation of an acetone solution containing **6a**.

Crystallographic data of **4a**, **4b** and **6a** were collected at 183(2) K with Mo K_α radiation (λ = 0.7107 Å) that was graphite-monochromated on an Oxford Diffraction

CCD Xcalibur system with a Ruby detector. Suitable crystals were covered with oil (Infineum V8512, formerly known as Paratone N), placed on a nylon loop that is mounted in a CrystalCap Magnetic™ (Hampton Research) and immediately transferred to the diffractometer. The program suite CrysAlis^{Pro} was used for data collection, multi-scan absorption correction and data reduction.⁴⁸ Crystallographic data of **7** were collected at 100(2) K at the PXIII beamline of the SLS synchrotron with a radiation wavelength of 0.71255 Å. The data was integrated with the XDS software⁴⁹ and further processed with the CCP4⁵⁰ and POINTLESS⁵¹ software. The data has a low completeness because of the one-circle geometry at the beamline and the low symmetry. All structures were solved with direct methods using SIR97⁵² and were refined by full-matrix least-squares methods on F^2 with SHELXL-2014.⁵³

Bioassay/s to Assess Anti-parasitic Activity.

Some parasites were produced *in vivo* in or on animals. *Haemonchus contortus* and *Trichostrongylus colubriformis* (strongylid nematodes) were maintained in sheep, and *Dirofilaria immitis* (filarial nematodes) in dogs. *Rhipicephalus sanguineus* (tick) was maintained on dogs. All animal experiments were approved by the State of Fribourg, Switzerland, and supervised by the Animal Welfare Officer of Novartis Animal Health. Other parasites, that is, *Ctenocephalides felis* (flea) and *Lucilia cuprina* (fly), were produced *in vitro* and maintained on defibrinated cattle blood. All bioassays were performed by Novartis Animal Health employing industry-standard operating procedures.

Assay to test activity *in vitro* against *Haemonchus contortus* and *Trichostrongylus colubriformis*.

This method was conducted as described by Kaminsky et al. (2008).¹¹ In brief, freshly harvested and cleaned nematode eggs were seeded into a 96-well plate containing the test substances to be evaluated for anthelmintic activity. Each compound was tested by serial dilution in order to determine its minimum effective dose. The test compounds were embedded in an agar-based nutritive medium allowing the full development of eggs through to third stage larvae (L3). The plates were incubated for 6 days at 28 °C and 80% relative humidity. Egg hatching and ensuing larval development were recorded to identify a possible nematocidal activity.

Efficacy was expressed as a percentage of reduced egg hatch, reduced development of L3, or paralysis and death of larvae of all stages.

Activity *in vitro* against *Dirofilaria immitis*

Microfilariae present in blood from donor dogs chronically infected with *D. immitis* were seeded into 96-well microplates. Individual test compounds were tested by serial dilution to determine their minimum effective doses. The plates were incubated for 48 h at 26 °C and 60% relative humidity. The motility of microfilariae was then recorded to identify any anti-filarial activity. Efficacy was expressed as the percentage of reduced motility compared to the control (untreated) and standards. In these assays, a compound needed to exhibit a nematocidal efficacy of > 60% at a concentration of 32 µg/ml (32 ppm) to qualify for further testing.

Activity *in vitro* against *Ctenocephalides felis*.

Oral test

This test was conducted as described by Wade et al. (1988) and Zakson-Aiken et al. (2001).^{54,55} In brief, adult fleas were placed in a suitably formatted microtitration plate, allowing fleas to access and feed on treated blood via an artificial feeding system. Each compound was tested by serial dilution to determine its minimum effective doses. Fleas were fed on treated blood for 24 h, after which the compound's effect was recorded. Insecticidal activity was determined on the basis of the number of dead fleas recovered from the feeding system.

Contact test

This test was conducted as described by Wade et al. (1988) and Zakson-Aiken et al. (2001).^{54,55} In brief, adult fleas were distributed into wells of a microplate pre-coated with a serial dilution of the compounds to be evaluated for insecticidal activity. The fleas were left in contact with the compound for 24 h. Insecticidal activity was confirmed upon death of the adult fleas. In these assays, a compound needed to exhibit an insecticidal efficacy of > 80% at a concentration of 100 ppm (100 µg/ml) to qualify for further testing.

Activity *in vitro* against *Rhipicephalus sanguineus* (dog tick).

Immersion test

This test was conducted as described by Lovis et al. (2011).⁵⁶ In brief, adult *Rhipicephalus sanguineus* were seeded into individual wells of a microtitration plate containing the test substances to be evaluated. Individual test compounds were tested by serial dilution to determine their minimum effective doses. Ticks were left in contact with the test compound for 10 min and then incubated at 28 °C and 80 % relative humidity for seven days, during which the test compounds' effects were monitored. Acaricidal activity was confirmed based on the pattern of lethality observed.

Contact (tarsal) test

This test was conducted as described by Lovis et al. (2013).⁵⁷ In brief, the test was performed by pre-coating wells of a 96-well microliter plate with a serial dilution of compound, allowing the evaluation of anti-parasitic activity by contact with ticks. Adult ticks were then distributed to individual wells of the plate and incubated at 28 °C and 80 % relative humidity for seven days, during which the test compound's effect was monitored. Acaricidal activity was confirmed upon death of the adult ticks.

Determination of ROS Level

The assay was performed following a procedure published by our group with slight modification.¹⁴ Briefly, HeLa cells (8000 in 100 μ L media/well) were seeded in a 96 well plate (Black, clear flat bottom from corning). Next day, the media was aspirated and 200 μ M fresh media containing **4a**, **4b**, **6a** or **6b** (freshly prepared stock solution in DMSO, after dilution with culture medium final concentration of DMSO \leq 0.3%, 25 μ M exposure concentration) was added. Cells were then incubated at 37 °C incubator for 20 h. The media was then removed, washed with 150 μ L PBS and then 150 μ L solution of H2DCFDA (final concentration 20 μ M) in serum free media was added and incubated for 40 min in dark. The fluorescence generated by intracellular ester cleavage followed by oxidation of H2DCFDA by intracellular ROS was quantified at 528 nm emission with 485 nm excitation wavelength in a SpectraMax M5 microplate Reader. For the positive control TBH, 100 μ M concentration and 6 h incubation time was used. After quantification of the ROS, cell viability on HeLa cells was determined to quantify the potential decrease in cellular mass due to treatment with

different compounds. The media was aspirated and cells were washed with 150 μ L PBS. Afterwards, 100 μ L 0.4% formaldehyde in PBS was added and cells were allowed to fix for 20 min at room temperature. The formaldehyde solution was aspirated and cells were washed with 150 μ L PBS. 0.02% of crystal violet (CV) solution in PBS was then added (100 μ L/well) and incubated at room temperature for 30 min. The CV solution was then aspirated, washed with 150 μ L of distilled water and dried overnight. Next day, 180 μ L 80% ethanol was added to each well and the plates were gently shaken on a rocker for 2-3 h and were read at 570 nm in a SpectraMax M5 microplate reader. The results expressed as mean and standard error of six replicates, corrected for the viable cell population.

Cell culture.

Human cervical carcinoma cells (HeLa) cells were cultured in DMEM (Gibco) supplemented with 5% fetal calf serum (FCS, Gibco), 100 U/ml penicillin, 100 μ g/ml streptomycin at 37 °C and 5% CO₂. The normal human fetal lung fibroblast MRC-5 cell line was maintained in F-10 medium (Gibco) supplemented with 10% FCS (Gibco), penicillin (100 U/ml), and streptomycin (100 μ g/ml).

Cytotoxicity Studies.

Cytotoxicity studies were performed on two different cell lines, namely HeLa, and MRC-5, by a fluorometric cell viability assay using Resazurin (Promocell GmbH). Briefly, one day before treatment, cells were seeded in triplicates in 96-well plates at a density of 4 x 10³ cells/well for HeLa and 7 x 10³ for MRC-5 in 100 μ l growth medium. Upon treating cells with increasing concentrations of organometallic-monepantel derivatives for 48 h, the medium was removed, and 100 μ l complete medium containing Resazurin (0.2 mg/ml final concentration) were added. After 4h of incubation at 37 °C, fluorescence of the highly red fluorescent product Resorufin was quantified at 590 nm emission with 540 nm excitation wavelength in a SpectraMax M5 microplate Reader.

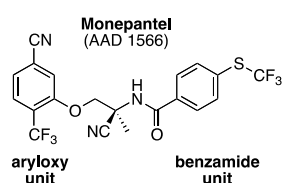
Supporting Information

^1H , ^{13}C and ^{19}F NMR spectra (**4a/b**, **5a/b**, **6a/b** and **7**), ORTEP plot of **7**, Anti-parasitic activity against *C. felis*, *L. cuprina* and *R. sanguineus* of organometallic precursors and derivatives (**4a/b**, **5a/b**, **6a/b** and **7**) (Table S1).

Acknowledgements

This work was financially supported by the Swiss National Science Foundation (Professorships N° PP00P2_133568 and PP00P2_157545 to G.G), the University of Zurich (G.G, S.F.), the Stiftung für wissenschaftliche Forschung of the University of Zurich (G.G, S.F.), the Novartis Jubilee Foundation (G.G), the Kurt u. Senta Hermann Stiftung (S.F.) and the Swiss Government Excellence Scholarship for Postdoctoral Researcher (R.L.). R.B.G.'s research program is supported by the Australian Research Council (ARC), the National Health and Medical Research Council (NHMRC), Melbourne Water Corporation, Yourgene Bioscience, the Alexander von Humboldt Foundation and The University of Melbourne. R.B.G. is a grateful recipient of Professorial Humboldt Research Awards. The authors would like to thank Dr. Jacques Bouvier (Novartis Animal Health, St-Aubin, Switzerland) and Dr. Noëlle Gauvry (Novartis Animal Health, Basel, Switzerland) for their help with the biological assays.

TOC



Inactive against *H. contortus*
and *T. colubriformis*

s

Ferrocenyl and ruthenocenyl derivatives of the nematocidal drug monepantel show organometallic-dependent activity against *H. contortus* and *T. colubriformis*.

References

- (1) Ducray, P.; Gauvry, N.; Pautrat, F.; Goebel, T.; Fruechtel, J.; Desaulles, Y.; Weber, S. S.; Bouvier, J.; Wagner, T.; Froelich, O.; Kaminsky, R. *Bioorg. Med. Chem. Lett.* **2008**, *18*, 2935.
- (2) Hess, J.; Konatschnig, S.; Morard, S.; Pierroz, V.; Ferrari, S.; Spingler, B.; Gasser, G. *Inorg. Chem.* **2014**, *53*, 3662.
- (3) Kaminsky, R.; Rufener, L.; Bouvier, J.; Lizundia, R.; Schorderet Weber, S.; Sager, H. *Vet. Parasitol.* **2013**, *195*, 286.
- (4) Gordon, C. P.; Hizartzidis, L.; Tarleton, M.; Sakoff, J. A.; Gilbert, J.; Campbell, B. E.; Gasser, R. B.; McCluskey, A. *MedChemComm* **2014**, *5*, 159.
- (5) *For legal issues the efficacy of AAD96 cannot be disclosed.*
- (6) Kaplan, R. M.; Vidyashankar, A. N. *Vet. Parasitol.* **2012**, *186*, 70.
- (7) Kaplan, R. M. *Trends Parasitol* **2004**, *20*, 477.
- (8) Howell, S. B.; Burke, J. M.; Miller, J. E.; Terrill, T. H.; Valencia, E.; Williams, M. J.; Williamson, L. H.; Zajac, A. M.; Kaplan, R. M. *Journal of the American Veterinary Medical Association* **2008**, *233*, 1913.
- (9) Mortensen, L. L.; Williamson, L. H.; Terrill, T. H.; Kircher, R. A.; Larsen, M.; Kaplan, R. M. *J. A. Vet. Med. Assoc.* **2003**, *23*, 495.
- (10) Epe, C.; Kaminsky, R. *Trends Parasitol.* **2013**, *29*, 129.
- (11) Kaminsky, R.; Ducray, P.; Jung, M.; Clover, R.; Rufener, L.; Bouvier, J.; Weber, S. S.; Wenger, A.; Wieland-Berghausen, S.; Goebel, T.; Gauvry, N.; Pautrat, F.; Skripsky, T.; Froelich, O.; Komoin-Oka, C.; Westlund, B.; Sluder, A.; Maser, P. *Nature* **2008**, *452*, 176.
- (12) Rufener, L.; Keiser, J.; Kaminsky, R.; Mäser, P.; Nilsson, D. *PLoS Pathog.* **2010**, *6*, e1001091.
- (13) Baur, R.; Beech, R.; Sigel, E.; Rufener, L. *Mol Pharmacol* **2015**, *87*, 96.
- (14) Rufener, L.; Bedoni, N.; Baur, R.; Rey, S.; Glauser, D. A.; Bouvier, J.; Beech, R.; Sigel, E.; Puoti, A. *PLoS Pathog* **2013**, *9*, e1003524.
- (15) Rufener, L.; Maeser, P.; Roditi, I.; Kaminsky, R. *PLoS Pathog.* **2009**, *5*, e1000380.
- (16) Van den Brom, R.; Moll, L.; Kappert, C.; Vellema, P. *Vet. Parasitol.* **2015**, *209*, 278.
- (17) Mederos, A.; Ramos, Z.; Banchemo, G. *Parasit Vectors* **2014**, *7*, 598.
- (18) Cezar, A. S.; Toscan, G.; Camillo, G.; Sangioni, L. A.; Ribas, H. O.; Vogel, F. S. F. *Vet. Parasitol.* **2010**, *173*, 157.
- (19) Scott, I.; Pomroy, W. E.; Kenyon, P. R.; Smith, G.; Adlington, B.; Moss, A. *Vet. Parasitol.* **2013**, *198*, 166.
- (20) Hess, J.; Patra, M.; Rangasamy, L.; Konatschnig, S.; Blacque, O.; Jabbar, A.; Mac, P.; Jorgensen, E. M.; Gasser, R. B.; Gasser, G. *J. Med. Chem* **2016**, submitted.
- (21) Hess, J.; Patra, M.; Pierroz, V.; Spingler, B.; Jabbar, A.; Ferrari, S.; Gasser, R. B.; Gasser, G. **2016**, to be submitted.
- (22) Gasser, G.; Metzler-Nolte, N. *Curr. Opin. Chem. Biol.* **2012**, *16*, 84.
- (23) Gasser, G.; Ott, I.; Metzler-Nolte, N. *J. Med. Chem* **2011**, *54*, 3.
- (24) Jaouen, G.; Metzler-Nolte, N. *Topics in Organometallic Chemistry*; Springer, 2010; Vol. 1.
- (25) Hartinger, C. G.; Dyson, P. J. *Chem. Soc. Rev.* **2009**, *38*, 391.

- (26) Bruijnincx, P. C. A.; Sadler, P. J. *Curr. Opin. Chem. Biol.* **2008**, *12*, 197.
- (27) Biot, C.; Glorian, G.; Maciejewski, L. A.; Brocard, J. S.; Domarle, O.; Blampain, G.; Millet, P.; Georges, A. J.; Abessolo, H.; Dive, D.; Lebibi, J. *J. Med. Chem.* **1997**, *40*, 3715.
- (28) Biot, C.; Dive, D. In *Medicinal Organometallic Chemistry*; Jaouen, G., Metzler-Nolte, N., Eds.; Springer-Verlag: Heidelberg, 2010; Vol. 32, p 155.
- (29) Biot, C.; Castro, W.; Botte, C. Y.; Navarro, M. *Dalton Trans.* **2012**, *41*, 6335.
- (30) Dive, D.; Biot, C. *ChemMedChem* **2008**, *3*, 383.
- (31) Rubbiani, R.; Blacque, O.; Gasser, G. *Dalton Trans.* **2016**.
- (32) Patra, M.; Gasser, G.; Wenzel, M.; Merz, K.; Bandow, J. E.; Metzler-Nolte, N. *Organometallics* **2010**, *29*, 4312.
- (33) Patra, M.; Gasser, G.; Pinto, A.; Merz, K.; Ott, I.; Bandow, J. E.; Metzler-Nolte, N. *ChemMedChem* **2009**, *4*, 1930.
- (34) Patra, M.; Ingram, K.; Pierroz, V.; Ferrari, S.; Spingler, B.; Gasser, R. B.; Keiser, J.; Gasser, G. *Chem. Eur. J.* **2013**, *19*, 2232.
- (35) Patra, M.; Ingram, K.; Pierroz, V.; Ferrari, S.; Spingler, B.; Keiser, J.; Gasser, G. *J. Med. Chem.* **2012**, *55*, 8790.
- (36) Patra, M.; Ingram, K.; Leonidova, A.; Pierroz, V.; Ferrari, S.; Robertson, M. N.; Todd, M. H.; Keiser, J.; Gasser, G. *J. Med. Chem.* **2013**, *56*, 9192.
- (37) Dubar, F.; Egan, T. J.; Pradines, B.; Kuter, D.; Ncokazi, K. K.; Forge, D.; Paul, J.-F. o.; Pierrot, C.; Kalamou, H.; Khalife, J.; Buisine, E.; Rogier, C.; Vezin, H.; Forfar, I.; Slomianny, C.; Trivelli, X.; Kapishnikov, S.; Leiserowitz, L.; Dive, D.; Biot, C. *ACS Chem. Biol.* **2011**, *6*, 275.
- (38) Chavain, N.; Vezin, H.; Dive, D.; Touati, N.; Paul, J.-F.; Buisine, E.; Biot, C. *Mol. Pharmaceutics* **2008**, *5*, 710.
- (39) Gouvry, N.; Goebel, T.; Ducray, P.; Pautrat, F.; Kaminsky, R.; Jung, M. **2005**, *142*, 481750.
- (40) Bernstein, J.; Davis, R. E.; Shimoni, L.; Chang, N. L. *Angew. Chem. Int. Ed.* **1995**, *34*, 1555.
- (41) Top, S.; Vessières, A.; Leclercq, G.; Quivy, J.; Tang, J.; Vaissermann, J.; Huché, M.; Jaouen, G. *Chem. Eur. J.* **2003**, *9*, 5223.
- (42) Biot, C.; Glorian, G.; Maciejewski, L. A.; Brocard, J. *J. Med. Chem.* **1997**, *40*, 3715.
- (43) Jaouen, G.; Top, S.; Vessières, A.; Leclercq, G.; McGlinchey, M. J. *Curr. Med. Chem.* **2004**, *11*, 2505.
- (44) Armarego, W. L. F.; Perrin, D. D. *Purification of Laboratory Chemicals*; 4th ed.; Butterworth-Heinemann: Oxford (UK), 1996.
- (45) Cormode, D. P.; Evans, A. J.; Davis, J. J.; Beer, P. D. *Dalton Trans.* **2010**, *39*, 6532.
- (46) Gottlieb, H. E.; Kotlyar, V.; Nudelman, A. *J. Org. Chem.* **1997**, *62*, 7512.
- (47) Fulmer, G. R.; Miller, A. J. M.; Sherden, N. H.; Gottlieb, H. E.; Nudelman, A.; Stoltz, B. M.; Bercaw, J. E.; Goldberg, K. I. *Organometallics* **2010**, *29*, 2176.
- (48) Agilent Technologies; 171.37 ed. Oxford, UK, 2014, p Xcalibur CCD system.
- (49) Kabsch, W. *Acta Cryst.* **2010**, *D66*, 125.
- (50) Bailey, S. *Acta Cryst.* **1994**, *D50*, 760.

- (51) Evans, P. R. *Acta Cryst.* **2011**, D67, 282.
- (52) Altomare, A.; Burla, M. C.; Camalli, M.; Cascarano, G. L.; Giacovazzo, C.; Guagliardi, A.; Moliterni, A. G. G.; Polidori, G.; Spagna, R. *J. Appl. Cryst.* **1999**, 32, 115.
- (53) Sheldrick, G. M. *Acta Cryst.* **2015**, C71, 3.
- (54) Zakson-Aiken, M.; Gregory, L. M.; Meinke, P. T.; Shoop, W. L. *J. Med. Entomol.* **2001**, 38, 576.
- (55) Wade, S. E.; Georgi, J. R. *J. Med. Entomol.* **1988**, 25, 186.
- (56) Lovis, L.; Perret, J. L.; Bouvier, J.; Fellay, J. M.; Kaminsky, R.; Betschart, B.; Sager, H. *Vet. Parasitol.* **2011**, 182, 269.
- (57) Lovis, L.; Mendes, M. C.; Perret, J. L.; Martins, J. R.; Bouvier, J.; Betschart, B.; Sager, H. *Vet. Parasitol.* **2013**, 191, 323.

Minerva Access is the Institutional Repository of The University of Melbourne

Author/s:

Hess, J; Patra, M; Jabbar, A; Pierroz, V; Konatschnig, S; Spingler, B; Ferrari, S; Gasser, RB;
Gasser, G

Title:

Assessment of the nematocidal activity of metallocenyl analogues of monepantel

Date:

2016-01-01

Citation:

Hess, J., Patra, M., Jabbar, A., Pierroz, V., Konatschnig, S., Spingler, B., Ferrari, S., Gasser, R. B. & Gasser, G. (2016). Assessment of the nematocidal activity of metallocenyl analogues of monepantel. DALTON TRANSACTIONS, 45 (44), pp.17662-17671.
<https://doi.org/10.1039/c6dt03376h>.

Persistent Link:

<http://hdl.handle.net/11343/123770>

File Description:

Submitted version